Stability and Spectroscopy of Single Nitrogen Dopants in Graphene at Elevated Temperatures

Jamie H. Warner,*,† Yung-Chang Lin,‡ Kuang He,† Masanori Koshino,‡ and Kazu Suenaga*,‡

†Department of Materials, University of Oxford, Parks Road, Oxford, OX1 3PH, U.K. and ‡Nanotube Research Center, National Institute of Advanced Industrial Science and Technology (AIST), Central 5, 1-1-1 Higashi, Tsukuba, Ibaraki 305-8565, Japan

ABSTRACT Single nitrogen (N) dopants in graphene are investigated using atomic-resolution scanning transmission electron microscopy (STEM) combined with electron energy loss spectroscopy (EELS). Using an *in situ* heating holder at 500 °C provided us with clean graphene surfaces, and we demonstrate that isolated N substitutional atoms remain localized and stable in the graphene lattice even during local sp^2 bond reconstruction. The high stability of isolated N dopants enabled us to acquire 2D EELS maps with simultaneous ADF-STEM images to map out the local bonding variations. We show that a substitutional N dopant causes changes in the EELS of the carbon (C) atoms it is directly bonded to. An upshift in the π^* peak of the C K-edge EELS of ~0.5 eV is resolved and supported by density functional theory simulations.

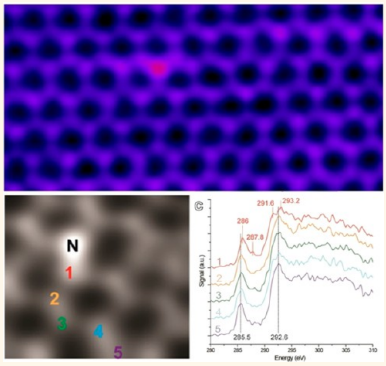

KEYWORDS: graphene · N-doped · STEM · EELS · aberration-corrected · nitrogen

Doping graphene with foreign elements is one approach to modifying its conductive properties, which is crucial for its further development in electronic applications.[1−8] Dopants can either reside on the surface of graphene, as adatoms, or be covalently bonded within the lattice. Surface adatom doping is common, simple to perform, but often unstable due to chemical reactivity with atmospheric molecules. Covalently bonded dopants are much more promising, as they are known to be stable against oxidation and hence offer a more permanent solution to graphene engineering.[9,10] Doping graphene with nitrogen or boron has attracted attention because of the analogy to 2D boron nitride materials and their hybridization with graphene.[1,11,12] Most experimental work has focused on N doping due to its easier experimental implementation compared to B doping. Prior to doping graphene with N, there have been considerable efforts to dope carbon nanotubes with N atoms.[13,14]

A key aspect of correctly predicting the property changes due to N dopants in graphene is to know the accurate atomic structural models. Low-voltage aberration-corrected (scanning) transmission electron microscopy (AC-STEM and AC-TEM) is now capable of imaging single-atom dopants in graphene with elements ranging from light atoms such as B and N to heavier atoms such as Fe and Si.[15−18] Atomic resolution images from AC-STEM and AC-TEM have enabled accurate atomic models to be generated for substitutional N-doped graphene,[19,20] substitutional Fe/Si-doped graphene,[15,21] and interstitial Fe/Si-doped graphene.[21] Time-dependent imaging has also revealed the dynamics of dopant atoms in graphene and their behavior during bond rotations and electron beam induced atomic sputtering.[21] Further insights about the local bonding states have been acquired by combining AC-STEM with electron energy loss spectroscopy using an angstrom-sized probe to obtain information from single atoms.[22] Atomic resolution spectroscopic maps have been obtained for single N atoms substituted in graphene demonstrating spatial correlation between a single high-contrast atom in the lattice of graphene and the N K-edge EELS signal. Bangert and co-workers demonstrated this for graphene implanted with

* Address correspondence to jamie.warner@materials.ox.ac.uk, Suenaga-kazu@aist.go.jp.

Received for review September 26, 2014 and accepted November 7, 2014.

Published online November 12, 2014
10.1021/nn5054798

N atoms that formed single-substituted dopants,[23] while Krivanek and co-workers demonstrated this for impurity N atoms in graphene.[24] In both cases, little attention was paid to the specific fine details of the EELS profiles, especially shifts in the C K-edge peak values. Recent simulations predict that the C K-edge EELS should be different for the C atoms surrounding a N dopant compared to normal graphene, with the emergence of a new peak between the π^* and σ^* peaks and a red shift of both the π^* and σ^* peaks.[25] Some evidence for a new peak in the K-edge EELS from N doping has been claimed, but the absence of any N K-edge EELS signal makes the element assignment of the higher contrast atom observed in AC-STEM uncertain.[25] Furthermore, none of the shifts in the π^* and σ^* peaks in the C K-edge EELS predicted by DFT were detected for the C atoms around the dopant.[25]

In this report, we use atomic-resolution AC-STEM and EELS to locate single N substitutional dopants in graphene by the presence of a N K-edge EELS signal and correlated single-atom high contrast in AC-STEM images. 2D EELS maps are acquired with simultaneous atomic-resolution annular dark field STEM (ADF-STEM) images. We extract the carbon K-edge EELS from various regions in the 2D EELS map corresponding to different locations with respect to the N dopant and examine the changes in the position of the π^* and σ^* peaks in the C K-edge EELS. We compare our experimental EELS profiles to DFT-based EELS simulations and find excellent agreement. The ability to unambiguously identify a single N atom dopant enabled us to track its dynamics during bond rotations and lattice reconstruction, revealing insights into the stability of single N atom dopants at elevated temperatures. This has important consequences for high-temperature processing of N-doped graphene, which is often required for surface cleaning.

RESULTS/DISCUSSION

Graphene was produced by chemical vapor deposition on a liquid Cu catalyst surface and transferred onto SiN TEM grids, followed by extensive cleaning. Nitrogen dopants were found incorporated within defective regions of graphene and near the edges of holes in graphene. No intentional doping of graphene with N atoms was undertaken at any stage. The N dopants could come from either exposure to the atmosphere or the SiN TEM grid. Our main focus in this report is on the structure, dynamics, and spectroscopy of the N dopants and surrounding C atoms and not on methods to synthesize N-doped materials. AC-STEM and EELS were performed at an accelerating voltage of 60 kV and using a sample heating holder set to 500 °C. Medium-angle annular dark field (MAADF) imaging condition was employed to enhance the contrast of light elements. Performing the experiments at high temperature resulted in the evaporation of the majority of surface residues and left a near-pristine clean surface. This was essential, as it allowed repeated imaging and spectroscopy of graphene regions without causing beam-induced contamination.

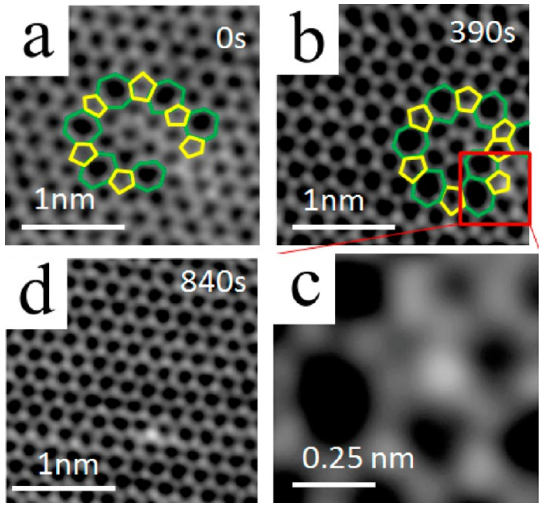

Figure 1. ADF-STEM images of a N atom in graphene lattice as a function of time. (a, b, and c) N atom with brighter contrast in a defective area of graphene. (d) After relaxation of the defect structure by bond rotation to leave a single N atom in graphene.

Atoms that exhibit increased contrast in ADF-STEM images were often observed in defective regions of graphene and at the edges. EELS on several of these atoms showed they are nitrogen. Figure 1a shows a flower-like defect in graphene formed primarily by several bond rotations. Within the bottom right of the defect a stronger contrast atom is visible, shown in Figure 1b and in higher magnification in Figure 1c. The strong contrast atom has substituted a single carbon atom and is in a five-membered ring. After electron beam irradiation for several minutes the defect structure disappeared and a single strong contrast atom remained as a substitutional dopant in graphene, Figure 1d. The initial defect structure in Figure 1a actually contains two excess atoms in the lattice and is not a vacancy from missing atoms. Defect structures from excess atoms in the lattice of graphene (without the N dopant) were recently reported in investigations into inflating graphene by atomic-scale blisters.[26] This defect structure is known to be susceptible to losing its 2+ atoms through electron beam irradiation, and this then leads to the transformation into the single N dopant. This reveals that the N atom remains after two carbon atoms have been sputtered from the lattice. The presence of excess atoms within this defect structure suggests that the N atom might have been one of the two original excess atoms incorporated into the defect structure, explaining how a single N substitutional dopant can arise within the bulk lattice region of pristine graphene. This sequence of images shows that N dopants remain stable in the lattice of graphene at 500 °C even during bond rotations and atom sputtering.

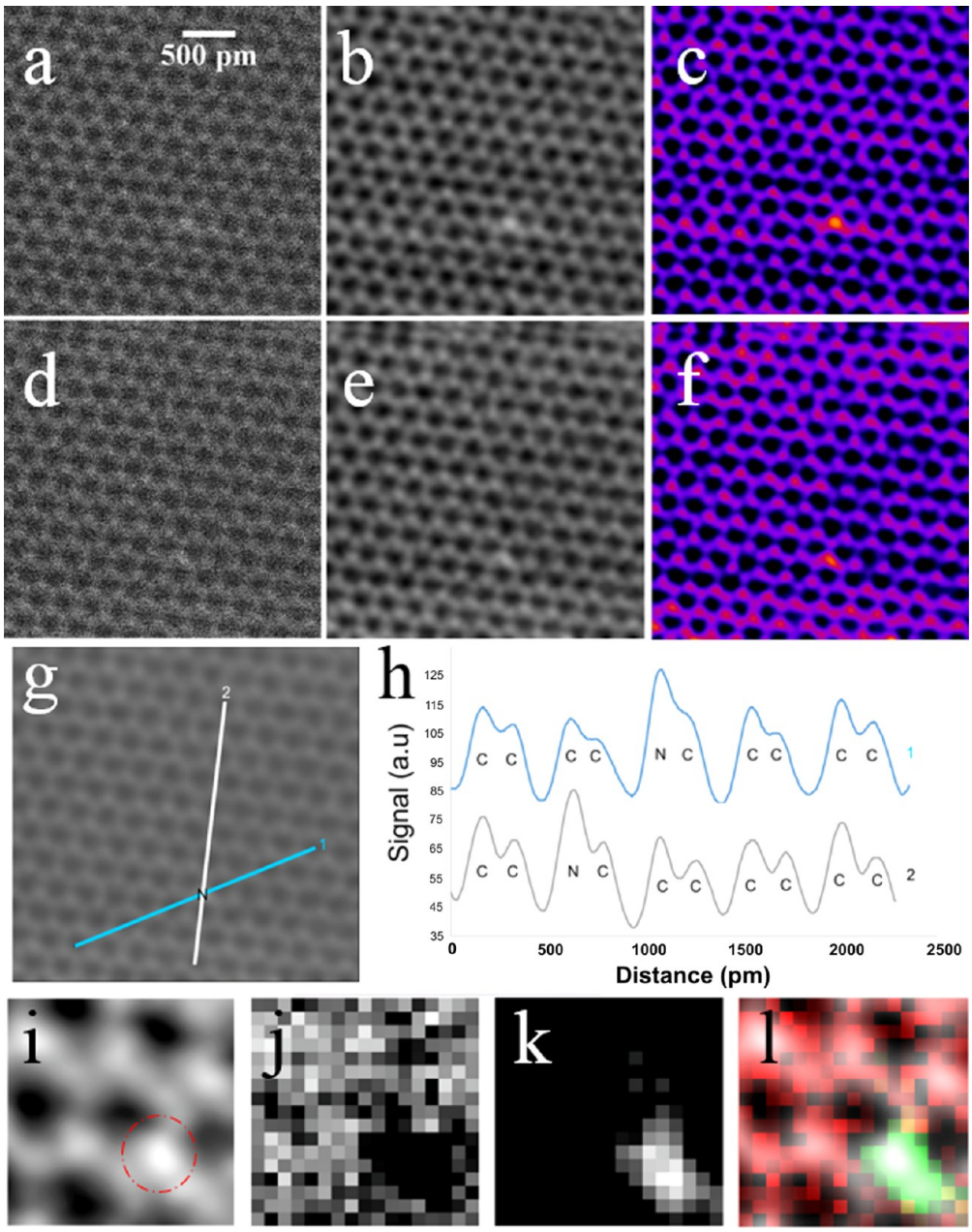

Figure 2. (a) Unprocessed ADF-STEM image of the N dopant in graphene from Figure 1d. (b) Smoothed ADF-STEM image of (a). (c) Use of color look-up table "fire" for (b) to show the increased contrast of the foreign atom. (d) Unprocessed ADF-STEM image of the same area as (a) but taken 1 min later. (e) Smoothed image of (d). (f) Color version of (e). (g) ADF-STEM image from (e) with white and blue lines showing where the line profiles of intensity are taken. (h) Plot of intensity line profiles from the two regions in (g). (i) ADF-STEM image taken simultaneously as a 2D EELS map over the region containing the high contrast atom in (a) and (d). (j) 2D spectroscopic map based on the C K-edge EELS. (k) 2D spectroscopic map based on the N K-edge EELS signal. (l) Overlap of C EELS map (red) and N EELS map (green) with ADF-STEM image.

For an ADF-STEM image the nitrogen atom should have increased contrast. Figure 2a shows the unprocessed ADF-STEM image and in Figure 2b the same image after smoothing, with Figure 2c utilizing a color look-up table to show the increased contrast. The same area was imaged 1 min later, and the ADF-STEM image is shown in Figure 2d–f, confirming the high contrast atom remains fixed. Line profiles across the N atom are taken in Figure 2g and presented in Figure 2h. The increased contrast from the N atom is detected, but because of the amount of noise in the original image, the accurate comparison of the N contrast *vs* the C contrast is not reliable. This can be seen in Figure 2h, where the contrast values vary slightly for the C atoms, but overall, we can conclude that the average contrast increase for the N atom is between 1.2 and 1.5, which is within range of the expected value of 1.3. A small amount of residual astigmatism is present that complicates this analysis. Instead we can conclusively confirm that the high contrast atom is a single N atom

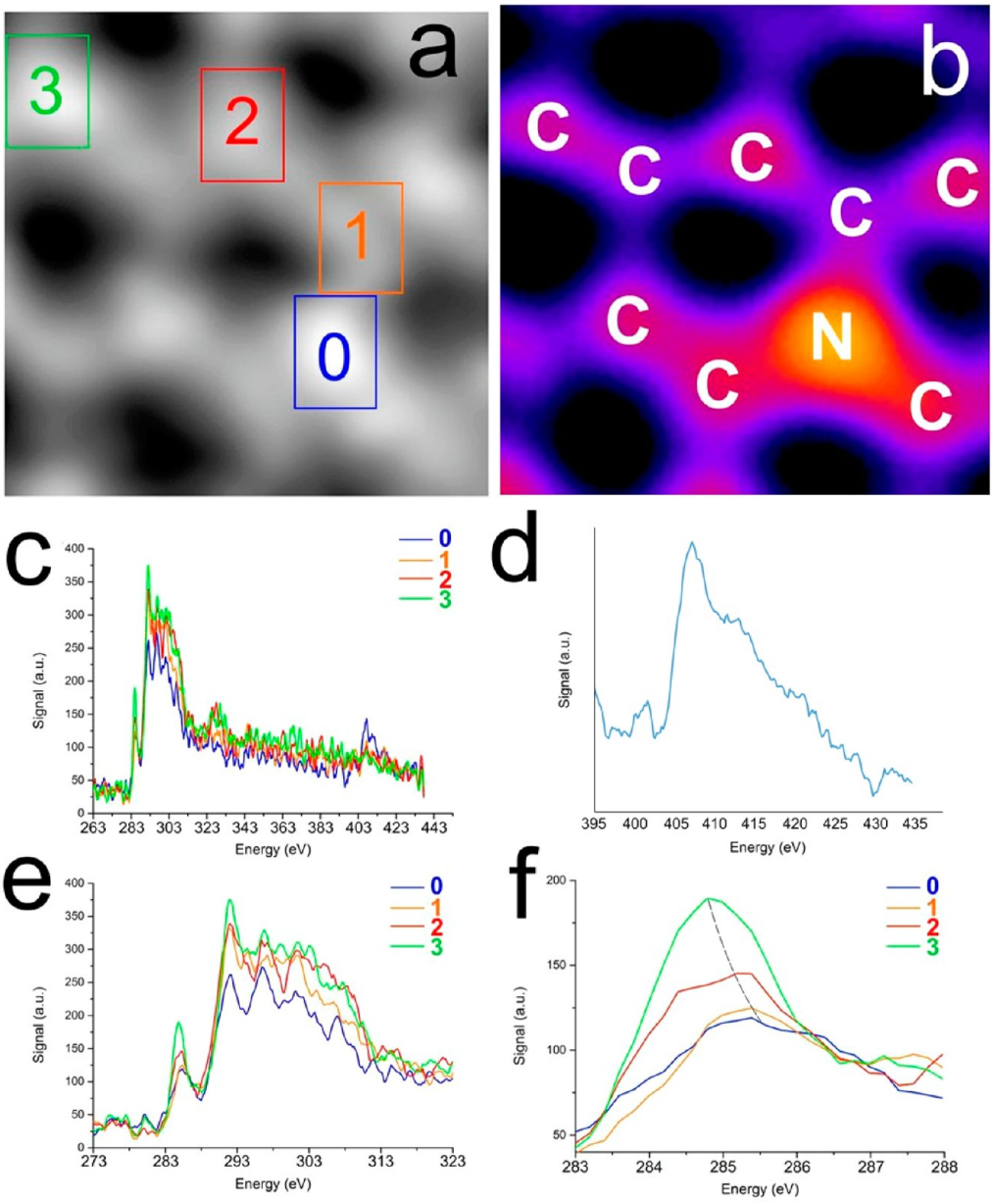

Figure 3. (a) ADF-STEM image taken simultaneously with the EELS map. Same image as in Figure 2i. (b) ADF-STEM image with high signal-to-noise of the same N dopant in graphene. (c) EELS corresponding to the boxed regions indicated in (a). (d) N K-edge EELS from averaging three different spectra taken from different areas containing single N substitutional dopants. (e) C K-edge region of the EELS corresponding to boxed regions in (a). (f) π^* region of the C K-edge EELS corresponding to the boxed regions in (a).

by analyzing the 2D EELS maps taken around the high contrast atom. This is more compelling than intensity profiles from ADF-STEM images, as the spectroscopic signature from EELS is quite definitive.

Figure 2i shows the ADF-STEM image taken simultaneously with a 2D EELS map, where the high contrast N atom is indicated by the dashed red circle. From the 2D EELS map, the signal associated with the C K-edge spectroscopic region (~280−320 eV) was used to generate the C map in Figure 2j and the signal from the N K-edge region (~400−430 eV) was used to generate the N map in Figure 2k. Figure 2l overlaps these two elemental maps with the ADF-STEM image from Figure 2i to show the correlation between the N signal and the single bright contrast atom. Given that the C K-edge EELS signal drops dramatically at the same location that the N K-edge EELS increases dramatically, informs us that there is no C atom underneath the N atom, and therefore the N atom is a direct substitution for a single C atom.

The 2D EELS map with correlated ADF-STEM images enables the extraction of the spatial locations of EELS signals to understand how the spectrum changes with different atomic positions. Figure 3 shows more spectroscopic detail regarding the C K-edge and N K-edge EELS signals. Figure 3a is the ADF-STEM image taken

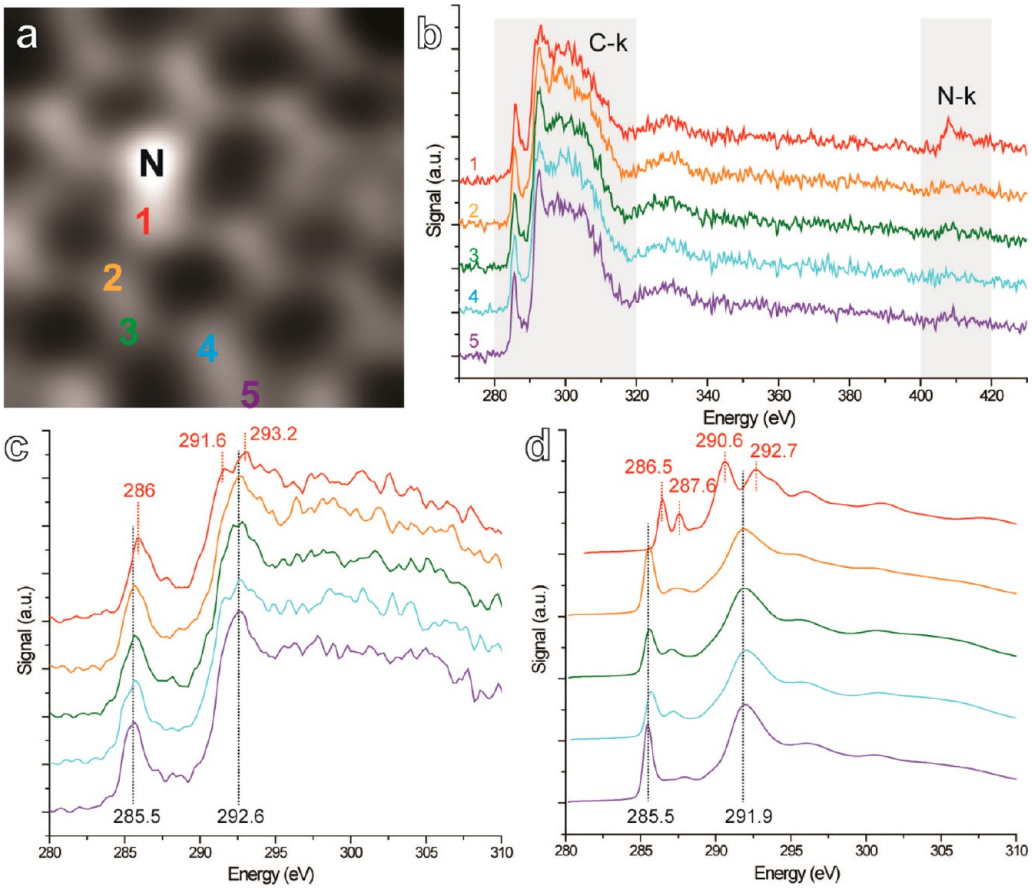

Figure 4. (a) ADF-STEM image of substitutional N dopant in graphene obtained simultaneously with the EELS map. EELS from the numbered atoms 1−5 from (a), showing both C K-edge and N K-edge regions. (c) EELS from the numbered atoms 1−5 from (a), showing only the C K-edge region. DFT-simulated EELS for equivalent atoms numbered 1−4 from (a) and 5 for pristine graphene model.

simultaneously with a 2D EELS map. To obtain EELS with decent signal-to-noise requires an increase in the integration time at each point, and this has the effect of taking longer to acquire the ADF-STEM image in Figure 3a compared to a normal single ADF-STEM image shown in Figure 3b of the same area. During the 2D EELS mapping there is some slight drift, and therefore the spatial resolution of the ADF-STEM image acquired at the same time, Figure 3a, is less than in Figure 3b, which is taken with a faster scan rate.

EELS from the boxed regions numbered in Figure 3a are presented in Figure 3c−f, with different energy resolution and regions explored. Figure 3c shows the N K-edge EELS signal from location 0, while all other atoms show just C K-edge signals. There is appreciable C K-edge EELS signal in location 0, and this is because of the inability to fully spatially separate the N atom from the neighboring C atoms and also from the delocalization effect in EELS measurements. In order to obtain a higher signal-to-noise N K-edge EELS, we average three EELS measurements taken of identical N substitutional dopants in different regions of the sample, shown in Figure 3d. This profile provides a clear signature for substitutional N dopants in graphene and matches the theoretical predicted EELS profile recently calculated for a N substitutional dopant.[27] Analysis of the C K-edge EELS shows some interesting results, Figure 3e and f. The C K-edge π^* peak shifts to higher energy (+0.6 eV) the closer the atoms are to the N atom. The σ^* signal drops in intensity, relative to the π^*, the closer the C atoms are to the N atom.

In order to confirm the shift in the π^* C K-edge peak is significant and not due to instability of the spectrometer, we examined around a second N atom substitutionally doped in graphene, Figures 4 and 5. The ADF-STEM image in Figure 4a was taken simultaneously with a 2D EELS map. The EELS from the C atoms numerically labeled in Figure 4a are shown in Figure 4b and c. The N K-edge signal is again observed for the bright atom in Figure 4a. Analysis of the C K-edge π^* region, Figure 4c, shows that the signal associated with atom 1 has an upshifted peak value compared to atoms 2−4. This confirms that the C atoms bonded to the single substitutional N atom have upshifted π^* peak and lower σ^* peak values. The shift in peaks is quite different from those observed for atoms at the edge of graphene, where typically new low-energy peaks below the π^* are detected.[22]

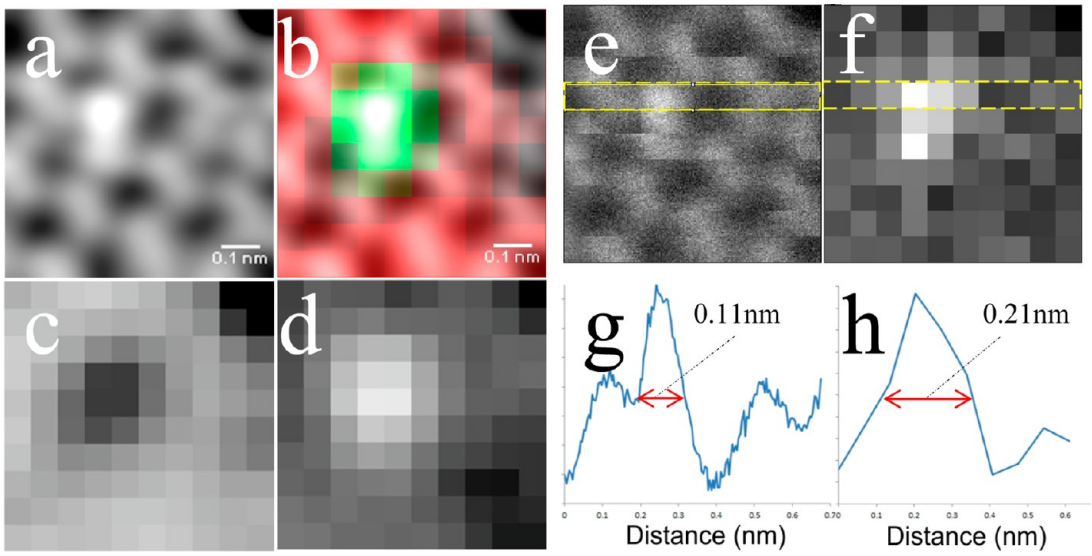

Figure 5. (a) ADF-STEM image (0.68 nm × 0.68 nm) taken simultaneously with the 2D EELS map. (b) Overlap of C K-edge EELS map (red) and N K-edge EELS map (green) with ADF-STEM image. (c) 2D spectroscopic map based on the C K-edge EELS (smoothed once). (d) 2D spectroscopic map based on the N K-edge EELS signal (smoothed once). (e) Unprocessed ADF-STEM image of (a) used for line profile analysis. (f) 2D spectroscopic EELS map (0.68 nm × 0.68 nm) using the N K-edge (without smoothing). (g) Boxed line profile of the ADF-STEM signal as a function of distance along the region indicated by the yellow box in (a). (h) Boxed line profile of the N K-edge EELS signal as a function of distance taken across the region indicated with a yellow box in (b).

The 2D spectroscopic maps in Figure 5a−d for C and N show that the single N atom replaced a single C atom in the lattice.

We performed density functional theory simulations of the C K-edge EELS for the equivalent atoms of 1−5 in the experimental data in Figure 4a, shown in Figure 4d. For atom 1 (red curve in Figure 4c and d), the DFT shows an upshift in the π^* peak of ∼1 eV, two new peaks at 287.6 and 290.6 eV, and an upshift of the σ^* peak of ∼0.8 eV. While there is a slight deviation in the quantitative values of the peak upshifts, the overall qualitative trends predicted by DFT are observed in the experimental data in Figure 4. These results confirm the upshifted π^* peak in the C K-edge EELS for atoms bonded to N in Figure 3f. The peak shifts in the C K-edge EELS appear strongest for the atoms directly bonded to the N atom.

The ability to acquire both 2D ADF-STEM images and 2D EELS maps enables a direct comparison between the full width at half-maximum (fwhm) of the two signals and provides information about the EELS delocalization effect in our measurement. Figure 5e shows the unprocessed ADF-STEM image that was originally presented in Figure 5a, with a yellow dashed box indicating the region for a line profile. Figure 5f shows the nonsmoothed N K-edge 2D spectroscopic image with the bright pixels coming from the same region as the ADF-STEM image. A yellow dashed box also indicates the region for line profile analysis. Figure 5g and h show the line profiles plotting (g) the ADF-STEM signal intensity and (h) the N K-edge EELS intensity as a function of distance. A double Gaussian fit to the ADF-STEM profile, Figure 5g, gave a fwhm for both the C and N atoms of 0.11 nm ± 0.01 nm, indicated with the red arrow. For Figure 5h, a single Gaussian fit gave a fwhm of 0.21 nm ± 0.03 nm shown with a red arrow, which is within a similar range to the values previously reported for a single Si dopant in graphene.[28] The fwhm of the ADF-STEM peak is as expected for the resolution of the microscope used and reflects the quality of the image in terms of the ability to resolve the peaks between the neighboring C and N atoms. Comparing this to the fwhm of the N K-edge EELS shows nearly twice the value. Since both the ADF-STEM image in Figure 5e and the EELS map in Figure 5f were acquired simultaneously, the difference in resolution is primarily due to the EELS delocalization effect.

In Figure 6 we plot the normalized ADF-STEM signal, N K-edge EELS signal, and the C K-edge EELS signal (from the same line profile location) all on the same distance axis. It shows that some N K-edge signal is still detected at the position of the C atom to the left of the N atom due to the delocalization effect. The fwhm of the N atom using K-edge EELS imaging measured in Figure 5 of ∼0.21 nm is right on the threshold of the spatial resolution required to resolve the position of C atoms in graphene (∼0.21 nm). This indicates that it is challenging to obtain 2D spectroscopic maps with lattice structure in graphene resolved, supporting the findings in ref 28. However, using a slower EELS line scan across graphene to achieve higher signal-to-noise can lead to the ability to resolve the C−C bond, as shown in Figure 6b. The two peaks labeled C−C in Figure 6b, regions 3 and 4, show where splitting can be seen in both the ADF-STEM image and the signal from the C K-edge EELS. Extending this to 2D EELS maps is

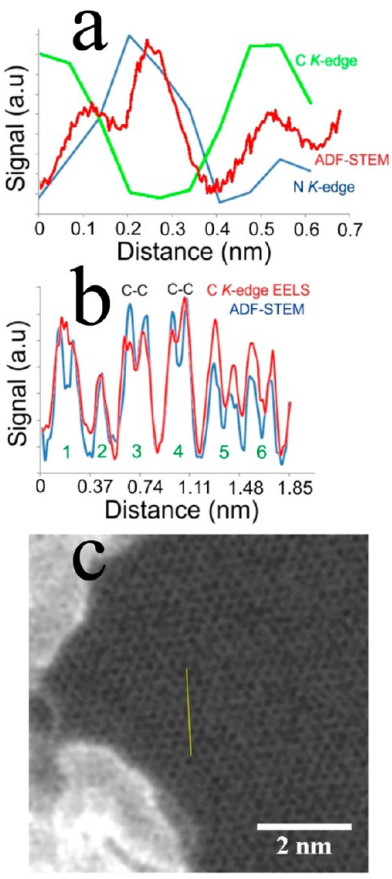

Figure 6. (a) Normalized plots of the line profile values obtained for the intensities of the C K-edge EELS, ADF-STEM signal, and the N K-edge EELS along the distances indicated in Figure 5e and f. (b) Comparison of ADF-STEM signal and C K-edge EELS signal for a slow line scan across graphene to achieve high signal-to-noise. The plot is broken into six different regions, labeled 1−6. Regions 3 and 4, labeled with C−C, show where both ADF-STEM and EELS line scan resolve the C−C bond. Two peaks are resolved within region 3, and two peaks resolved within region 4. The region of the line scan is shown in yellow in (c). (c) ADF-STEM image of monolayer graphene showing a yellow line used for a line scan EELS and ADF acquisition.

challenging due to the higher constraints placed on sample drift to achieve an image compared to a line profile. Even within the line scan in Figure 6b, some of the other peaks do not show splitting due to drift of the sample.

As mentioned previously, we noticed that the N dopants were primarily located either in defects or around edges. In Figure 7, we track the dynamics of a single N dopant in graphene during sp^2 bond reconstructions induced by the electron beam. We saw in Figure 1 that the N atom was stable during reconfiguration, and in Figure 7 we examine this in a second example with more frames capturing the dynamics of the transformation process. Figure 7a−h show a series of ADF-STEM images taken from a region containing a bright contrast atom, indicated with a white dashed circle. To confirm that the bright contrast atom is N, 2D EELS maps were taken in between some of the frames (Figure 7a−h). For example, after the ADF-STEM image in Figure 7d was taken, we acquired a 2D EELS map with a simultaneous ADF-STEM image of the same region (shown in Figure 7i). We then generated a N K-edge spectroscopic map, Figure 7j, showing the strong N signal located on the same position as the bright contrast spot, indicated with the dashed white circle. The EELS in Figure 7k shows the N K-edge signal from the N atom in Figure 7j. A similar study was done after Figure 7f to yield Figure 7l−n, and after Figure 7h to yield Figure 7o−q.

The time sequence in Figure 7 shows the N atom remains in the lattice throughout a sequence of bond rotations and lattice restructuring. Previous work showed that N atoms are stable within the lattice of graphene under electron beam irradiation at an accelerating voltage of 80 kV and at room temperature.[29] The final image in Figure 7h shows the N atom near the edge after beam-induced sputtering has increased the hole size. The N atom sits within a pentagon structure at the graphene edge. The N atom has remained in the same position, within a lattice spacing, throughout the reconstruction process, revealing that there is hardly any migration within the lattice at this temperature. These images show the high stability of the N atom during structural reconfiguration at elevated temperature of 500 °C.

In order to confirm the observations in Figure 7, we examined another case of a N dopant located near the edge during structural reconfiguration, Figure 8. Figure 8a shows a low-magnification ADF-STEM image with the yellow boxed region showing where the single N dopant is located. Figure 8b shows a high-magnification ADF-STEM image of this region, and the increased contrast from the N atom is observed (white dashed circle). The N atom is situated within a pentagon ring in Figure 8b. Another image taken 270 s later, Figure 8c, shows three atoms have been lost from the edge of graphene and a subsequent bond rotation has occurred. The N atom still remains relatively fixed in its position after this and is still situated in a pentagonal ring. After a further 55 s (Figure 8d), a couple of bond rotations have occurred, as well as the addition of one extra C atom to the edge, resulting in a full hexagonal lattice structure around the N dopant. Figure 8e−h show schematic atomic models that represent the structures observed in the ADF-STEM images in Figure 8b−d. We imaged this same region after a further 130 s, and the structure remained free from pentagonal rings around the N dopant, indicating that once the lattice reconstructs to hexagonal rings it remains stable in this configuration around the N dopant. Figure 8 confirms the findings in Figure 7, that substitutional N atoms are stable in the lattice and remain fixed in their location.

CONCLUSION

Our results have demonstrated that using a high-temperature *in situ* holder at 500 °C removes the

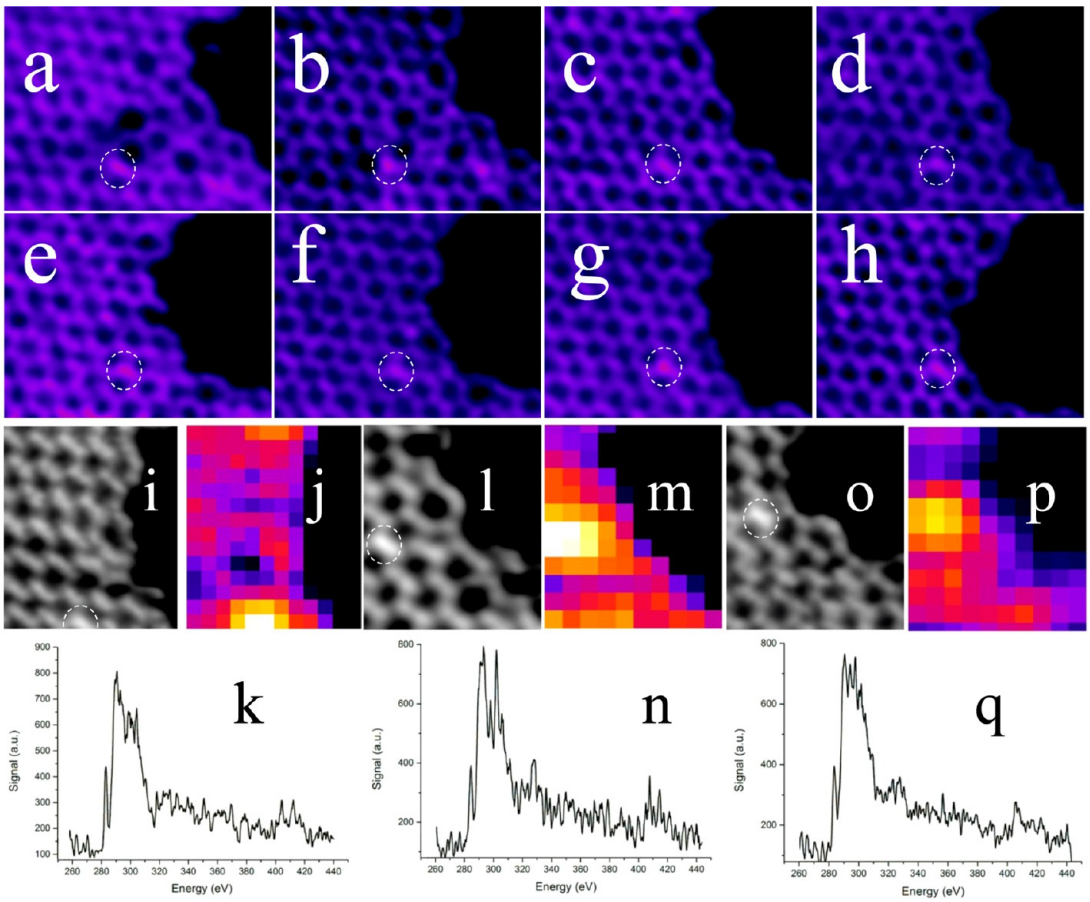

Figure 7. (a–h) Time series of ADF-STEM images capturing the dynamics of a single N atom in defects near the edge of graphene. White dashed circles indicate the location of the N atom. Time between images is ~20 s. (i) ADF-STEM image acquired simultaneously with 2D EELS map for (d), with a corresponding N K-edge EELS map in (j) and the EELS in (k) showing the presence of a N K-edge. (l) ADF-STEM image acquired simultaneously with a 2D EELS map for (f), with a corresponding N K-edge EELS map in (m) and the EELS in (n) showing the presence of a N K-edge. (o) ADF-STEM image acquired simultaneously with a 2D EELS map for (h), with a corresponding N K-edge EELS map in (p) and the EELS in (q) showing the presence of a N K-edge. The images in (i), (l), and (o) are not aligned.

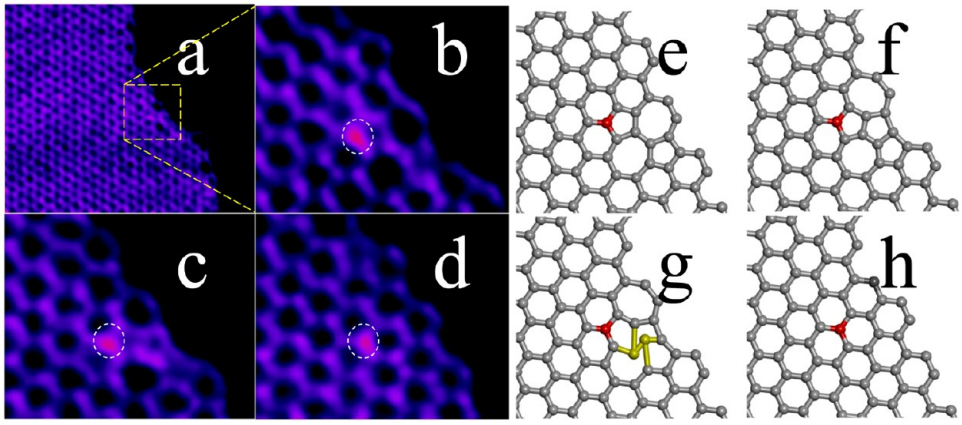

Figure 8. (a) ADF-STEM image of a region near the edge of graphene containing a single N dopant. (b) Higher magnification ADF-STEM image of the region indicated with the yellow box in (a), showing the single N atom, white dashed circle. (c) Same area as in (b) but taken after a further 270 s. (d) Same area as in (c), but taken after a further 60 s. (e) Atomic model for the image in (b). (f) Atomic model for the image in (c). (g) Atomic model showing the bond rotation (yellow) that helps convert the pentagonal rings to hexagonal rings. (h) Atomic model for image (d). Red atom in (e)–(h) indicates N atom.

surface contamination on graphene and enables clean surfaces for examination. We found isolated N dopants within the graphene that were direct substitutions for C atoms. These N dopants were extremely stable in the lattice and remain fixed in their position even during local sp^2 bond reconstruction. The N dopants were

readily observed within pentagonal rings and hexagonal rings. Detailed EELS of the single N dopants revealed new information about both the C and N K-edge spectra. C K-edge spectra showed a shift in the π^* peak for atoms around the N dopant, which matched DFT simulations. N K-edge spectra showed a unique profile that matched recent DFT simulations for isolated N substitutional dopants in graphene. These results provide detailed fundamental information that will influence our understanding of the EELS of N-doped C materials and the processing of N-doped graphene at elevated temperatures.

METHODS

Graphene Synthesis by CVD and Transfer to TEM Grids. Graphene was synthesized by atmospheric pressure chemical vapor deposition using molten copper as the catalyst under previously reported conditions.[21] Copper foil (99.999% purity, 0.1 mm thick Alfa Aesar) was placed onto a similarly sized Mo foil and loaded into a 1 in. quartz tube in a CVD furnace system. A gas flow of 100 sccm H_2/Ar (20% gas mix) and 200 sccm pure Ar was used to flush the system while the temperature ramps up to 1090 °C. The sample was then placed into the center of the hot furnace by sliding the quartz tube and then left to anneal for 30 min. Then CH_4 flow (1% gas mix in Ar) was introduced for 1 h at a flow rate of 10 sccm, with the H_2 set at 80 sccm. The sample was cooled and removed from the furnace. PMMA was spin-coated onto the surface, and the Cu metal etched away using $FeCl_3$. The graphene-PMMA is then washed several times in water and then transferred onto a SiN TEM grid with 2 μm holes. The PMMA was removed by burning in air overnight at 300 °C and then under vacuum overnight at ~180 °C.

Scanning Transmission Electron Microscopy. A JEM 2100F with a cold field emission source and DELTA-type aberration correctors was operated at 60 kV for STEM and EELS. The beam current was estimated at around 40 pA in a 0.1 nm probe. The convergence semiangle (α) was 35 mrad and the inner acquisition semiangle (β) was 62 mrad for the ADF imaging and EELS collection. Carbon K-edge ELNES analysis was performed with an energy dispersion of between 0.05 and 0.1 eV, and the acquisition time for each spectrum set to between 0.05 and 0.2 s. The zero loss width of the incident electron beam was about 0.35 eV. A JEOL high-temperature holder was used to heat the sample to 500 °C during imaging and spectroscopy to remove surface contaminations. EELS data were processed using the Cornell Spectrum Imager plugin in ImageJ.[30] ADF-STEM images were first smoothed using a Gaussian blur filter in ImageJ, followed by appropriate adjustment of brightness/contrast settings. Color images were generated by changing the look-up table from grayscale to "fire" in ImageJ.

Carbon K-Edge ELNES Simulations for Edge Structures of Graphene by All-Electron Band Calculation. The structure of graphene was initially modeled with a hexagonal structure ($a = b = 246.4$ pm, $c = 1280.33$ pm). A graphene sheet of a $3 \times 3 \times 1$ supercell with $P\bar{6}m2$ symmetry was created in order for a carbon atom with a core-hole to be well separated. For N-doped graphene, one of the carbon atoms in $3 \times 3 \times 1$ graphene is substituted by a nitrogen atom, maintaining three coordination with adjacent carbon atoms. The nitrogen atom and its neighboring carbon with a core-hole break the symmetry from $P\bar{6}m$ to $Amm2$ with parameters of $a = 671.10$, $b = 739.20$, $c = 1280.33$ pm, and $\alpha = \beta = \gamma = 90°$. A core-hole is introduced to a carbon atom in the graphene model and one of the carbon atoms adjacent to nitrogen in order to simulate carbon K-edge spectra.

We performed all-electron band calculation by using Wien2k code (version 12.1), based on the linearized augmented plane wave (LAPW) method.[31] The radius of the muffin tin sphere, R_{MT}, of carbon was set to 1.34 Å in the graphene model. The R_{MT} of carbon and nitrogen atoms were set to 1.30 and 1.37 Å for N-doped graphene. We use the Perdew–Burke–Ernzerhof generalized in the gradient approximation (PBE-GGA)[32] of the exchange–correlation potential with an energy separation of −6.0 Ry between core and valence states. The magnitude of the largest vector, G_{max}, was set to 12.0 Ry. The value of RK_{max}, which determines the number of basis functions (size of the matrices), was set to 7.0 Ry. E_{max}, the extension of energy levels for unoccupied DOS, was set to 2.5 Ry. The number of k-points was set to 1000 during the self-consistent field (SCF) iterations in which the convergence criterion was set to 0.0001 Ry. We did the SCF calculations without a core-hole (ground state) and with a core-hole (final state) for both graphene and N-doped graphene: one electron is removed from a frozen core state and added to the valence band.

The ELNES spectrum of the carbon K-edge was simulated by the TELNES3 program in Wien2k.[33] The k point is increased up to 1000 ($9 \times 10 \times 10$) for the ELNES simulation of N-doped graphene. The fwhm was set to $0.5 + 0.1 \times (\varepsilon_k - \varepsilon_{threshold})$ eV, where the fwhm increases with increasing energy differential between the threshold energy, $\varepsilon_{threshold}$, and the energy above the threshold, ε_k.[34] The experimental parameters were based on the present experimental conditions of 60 kV beam energy, 62.0 mrad collection angle, and 35.0 mrad convergence angle. The carbon K-edge ELNES with main and orbital quantum numbers, $n = 1$ and $\ell = 0$ was calculated, based on the final state selection rule of $\Delta\ell = \pm 1$. The threshold energy of the carbon K-edge was calculated from the energy difference, $E_{ground\text{-}state} - E_{final\text{-}state}$, where $E_{groun\text{-}state}$ and $E_{final\text{-}state}$ are the total energy with the electron configuration of the ground state and the final state (an electron removed from the 1 s band and added into the valence band during SCF calculations), respectively. As the π^* peak of the graphene model appears 5.6 eV higher in energy compared to that at 285.5 eV in the experiment, the threshold energy for each carbon is shifted 5.6 eV downward for better comparison.

Conflict of Interest: The authors declare no competing financial interest.

Acknowledgment. J.H.W. thanks the support from the Royal Society and the Sasakawa Fund. Y.C.L., M.K., and K.S. acknowledge support from the JST Research Acceleration Programme. Financial support by JSPS KAKENHI 23681026 and 26390004 is acknowledged by M.K.

REFERENCES AND NOTES

1. Wei, D.; Liu, Y.; Wang, Y.; Zhang, H.; Huang, L.; Yu, G. Synthesis of N-Doped Graphene by Chemical Vapor Deposition and Its Electrical Properties. *Nano Lett.* **2009**, *9*, 1752–1758.
2. Qu, L.; Liu, Y.; Baek, J.-B.; Dai, L. Nitrogen-Doped Graphene as Efficient Metal-Free Electrocatalyst for Oxygen Reduction in Fuel Cells. *ACS Nano* **2010**, *4*, 1321–1326.
3. Schedin, F.; Geim, A. K.; Morozov, S. V.; Hill, E. W.; Blake, P.; Katsnelson, M. I.; Novoselov, K. S. Detection of Individual Gas Molecules Adsorbed on Graphene. *Nat. Mater.* **2007**, *6*, 652–655.
4. Reddy, A. L. M.; Srivastava, A.; Gowda, S. R.; Gullapalli, H.; Dubey, M.; Ajayan, P. M. Synthesis of Nitrogen-Doped Graphene Films for Lithium Battery Application. *ACS Nano* **2010**, *4*, 6337–6342.
5. Giera, I.; Riedl, C.; Starke, U.; Ast, C. R.; Kern, K. Atomic Hole Doping of Graphene. *Nano Lett.* **2008**, *8*, 4603–4607.
6. Guo, B.; Liu, Q.; Chen, E.; Zhu, H.; Fang, L.; Gong, J. R. Controllabel N-Doping of Graphene. *Nano Lett.* **2010**, *10*, 4975–4980.
7. Wu, Z.-S.; Ren, W.; Xu, L.; Li, F.; Cheng, H.-M. Doped Graphene Sheets As Anode Materials with Superhigh Rate and Large Capacity for Lithium Ion Batteries. *ACS Nano* **2011**, *5*, 5463–5471.

8. Wang, Y.; Shao, Y.; Matson, D. W.; Li, J.; Lin, Y. Nitrogen-Doped Graphene and Its Application in Electrochemical Biosensing. *ACS Nano* **2010**, *4*, 1790–1798.
9. Lin, Y.-C.; Lin, C.-Y.; Chiu, P.-W. Controllable Graphene N-Doping with Ammonia Plasma. *Appl. Phys. Lett.* **2010**, *96*, 133110.
10. Wang, X.; Li, X.; Zhang, L.; Yoon, Y.; Weber, P. K.; Wang, H.; Guo, J.; Dai, H. N-Doping of Graphene through Electrothermal Reactions with Ammonia. *Science* **2009**, *324*, 768–771.
11. Sheng, Z.-H.; Gao, H.-L.; Bao, W.-J.; Wang, F.-B.; Xia, Xi.-H. Synthesis of Boron Doped Graphene for Oxygen Reduction Reaction in Fuel Cells. *J. Mater. Chem.* **2012**, *22*, 390–395.
12. Wang, H.; Maiyalagan, T.; Wang, X. Review on Recent Progress in Nitrogen-Doped Graphene: Synthesis, Characterization, and Its Potential Applications. *ACS Catal.* **2012**, *2*, 781–794.
13. Gong, K.; Du, F.; Xia, Z.; Durstock, M.; Dai, L. Nitrogen-Doped Carbon Nanotube Arrays with High Electrocatalytic Activity for Oxygen Reduction. *Science* **2009**, *323*, 760–763.
14. Tang, Y.; Allen, B. L.; Kauffman, D. R.; Star, A. Electrocatalytic Activity of Nitrogen-Doped Carbon Nanotube Cups. *J. Am. Chem. Soc.* **2009**, *131*, 13200–13201.
15. Zhou, W.; Kapetanakis, M. D.; Prange, M. P.; Pantelides, S. T.; Pennycook, S. J.; Idrobo, J.-C. Direct Determination of the Chemical Bonding of Individual Impurities in Graphene. *Phys. Rev. Lett.* **2012**, *109*, 206803.
16. Jin, C.; Lin, F.; Suenaga, K.; Iijima, S. Fabrication of a Freestanding Boron Nitride Single Layer and Its Defect Assignments. *Phys. Rev. Lett.* **2009**, *102*, 195505.
17. Ci, L.; Song, L.; Jin, C.; Jariwala, D.; Wu, D.; Li, Y.; Srivastava, A.; WANG, Z. F.; Storr, K.; Balicas, L.; *et al*. Atomic Layers of Hybridized Boron Nitride and Graphene Domains. *Nat. Mater.* **2010**, *9*, 430–435.
18. Wang, H.; Wang, Q.; Cheng, Y.; Li, K.; Yao, Y.; Zhang, Q.; Dong, C.; Wang, P.; Schwingenschlögl, U.; Yang, W.; *et al*. Doping Monolayer Graphene with Single Atom Substitutions. *Nano Lett.* **2012**, *12*, 141–144.
19. Meyer, J. C.; Kurasch, S.; Park, H. J.; Skakalova, V.; Künzel, D.; Gross, A.; Chuvilin, A.; Algara-Siller, G.; Roth, S.; Iwasaki, T.; *et al*. Experimental Analysis of Charge Redistribution due to Chemical Bonding by High-Resolution Transmission Electron Microscopy. *Nat. Mater.* **2011**, *10*, 209–215.
20. Zhao, L.; He, R.; Rim, K. T.; Schiros, T.; Kim, K. S.; Zhou, H.; Gutiérrez, C.; Chockalingam, S. P.; Arguello, C. J.; Pálová, L.; *et al*. Visualizing Individual Nitrogen Dopants in Monolayer Graphene. *Science* **2011**, *333*, 999–1003.
21. Robertson, A. W.; Montanari, B.; He, K.; Kim, J.; Allen, C. S.; Wu, Y. A.; Olivier, J.; Neethling, J.; Harrison, N.; Kirkland, A. I.; *et al*. Dynamics of Single Fe Atoms in Graphene Vacancies. *Nano Lett.* **2013**, *13*, 1468–1475.
22. Suenaga, K.; Koshino, M. Atom-by-Atom Spectroscopy at Graphene Edge. *Nature* **2010**, *468*, 1088–1090.
23. Bangert, U.; Pierce, W.; Kepaptsoglou, D. M.; Ramasse, Q.; Zan, R.; Gass, M. H.; Van den Berg, J. A.; Boothroyd, C. B.; Amani, J.; Hofsäss, H. Ion Implantation of Graphene-Toward IC Compatible Technologies. *Nano Lett.* **2013**, *13*, 4092–4097..
24. Krivanek, O. L.; Chisholm, M. F.; Murfitt, M. F.; Dellby, N. Scanning Transmission Electron Microscopy: Albert Crewe's Vision and Beyond. *Ultramicroscopy* **2012**, *123*, 90–98.
25. Nicholls, R. J.; Murdock, A. T.; Tsang, J.; Britton, J.; Pennycook, T. J.; Koós, A.; Nellist, P. D.; Grobert, N.; Yates, J. R. Probing the Bonding in Nitrogen-Doped Graphene Using Electron Energy Loss Spectroscopy. *ACS Nano* **2013**, *7*, 7145–7150.
26. Robertson, A. W.; He, K.; Kirkland, A. I.; Warner, J. H. Inflating Graphene with Atomic Scale Blisters. *Nano Lett.* **2014**, *14*, 908–914.
27. Arenal, R.; March, K.; Ewels, C. P.; Rocquefelte, X.; Kociak, M.; Loiseau, A.; Stephan, O. Atomic Configuration of Nitrogen-Doped Single-Walled Carbon Nanotubes. *Nano Lett.* **2014**, *14*, 5509−5516.
28. Zhou, W.; Oxley, M. P.; Lupini, A. R.; Krivanek, O. L.; Pennycook, S. J.; Idrobo, J.-C. Single Atom Microscopy. *Microsc. Microanal.* **2012**, *18*, 1342–1354.
29. Susi, T.; Kotakoski, J.; Arenal, R.; Kurasch, S.; Jiang, H.; Skakalova, V.; Stephan, O.; Krasheninnikov, A. V.; Kauppinen, E.; Kaiser, U.; Meyer, J. C. Atomistic Description of Electron Beam Damage in Nitrogen-Doped Graphene and Single-Walled Carbon Nanotubes. *ACS Nano* **2012**, *6*, 8837–8846.
30. Cueva, P.; Hovden, R.; Mundy, J. A.; Xin, H. L.; Muller, D. A. Data Processing for Atomic Resolution EELS. *Microsc. Microanal.* **2012**, *18*, 667–675.
31. Blaha, P.; Schwarz, K.; Sorantin, P.; Trickey, S. B. Full-Potential, Linearized Augmented Plane Wave Programs for Crystalline Systems. *Comput. Phys. Commun.* **1990**, *59*, 399–415.
32. Perdew, J. P.; Burke, K.; Ernzerhof, M. Generalized Gradient Approximation Made Simple. *Phys. Rev. Lett.* **1996**, *77*, 3865.
33. Jorissen, K. The *ab Initio* Calculation of Relativistic Electron Energy Loss Spectra. Doctor of Philosophy Thesis. Universiteit Antwerpen, 2007.
34. Hébert, C. Practical Aspects of Running the WIEN2k Code for Electron Spectroscopy. *Micron* **2007**, *38*, 12–28.